Wet-Chemical Synthesis and Physico / Electro-Chemical Performance Characteristics of Novel Perovskite Cathode Materials for Low-Temperature Solid Oxide Fuel Cells

***Reni, Mullukattil Lukose; Samson Nesaraj, A.* *+**

Department of Chemistry, Karunya Institute of Technology and Sciences,
(Deemed to be University) Karunya Nagar, Coimbatore – 641 114, Tamil Nadu, INDIA

ABSTRACT: *Different perovskite-based materials are proposed as cathode materials for solid oxide fuel cells (SOFCs) working at low temperatures (~600 °C). In this research work, a set of perovskite cathode materials, such as $Sm_{1-x}Ce_xCoO_{3-\delta}$, $Sm_{1-x}Ce_xMnO_{3-\delta}$, $Gd_{1-x}Ce_xCoO_{3-\delta}$ and $Gd_{1-x}Ce_xMnO_{3-\delta}$ (x = 0.1–0.2) were prepared for SOFC applications by co-precipitation method with sodium hydroxide solution as the precipitating agent. The precipitated hydroxides were calcined at 300, 600, 750, 900, and 1100 °C /2 hours in the air using a thermolyne furnace. The calcined powder particles were characterized by XRD, FT-IR, Particle Size, SEM, and EDAX techniques. XRD patterns revealed the presence of orthorhombic primitive phases in the samples. Crystallite sizes of the materials were also determined with XRD method. The presence of M-O bond was confirmed by FT-IR spectroscopy. Particle size analysis proved the presence of samples in the range of 247-976 nm. However, the SEM images revealed the presence of nano-sized particles. The atomic percentage of elements present in the materials was measured by EDAX. Pellets of cathode samples were made and sintered at high temperatures. The conductivity values of the specimens were measured with electrochemical impedance spectroscopy at different temperatures. The cathode specimen, $Gd_{1-x}Ce_xCoO_{3-\delta}$ (x=0.1 and 0.2) exhibited better electronic conductivity than other samples. It was found that the prepared cathode samples are stable at moderate temperatures and suitable for Low-Temperature Solid Oxide Fuel Cell (LTSOFC) application.*

KEYWORDS: *SOFC; Cathode; Nanoceramic materials; Conductivity studies.*

INTRODUCTION

Solid oxide fuel cells get research interest due to high energy conversion, low polluting emissions, and high choices of fuels. High temperature over 800 °C is required to maintain high oxygen – ionic conductivity in high-temperature solid oxide fuel cell [1]. Polarization resistance of cathode is the main contributor to overall cell resistance at intermediate operating temperature. Novel cathode materials are needed with high catalytic activities to enhance the generation rate of oxygen ions and to decrease the operating temperature [2]. The important

** To whom correspondence should be addressed.*
+ E-mail: drsamson@karunya.edu
1021-9986/2021/2/463-475 13/$/6.03

peculiarities of novel cathode materials are high rate of oxygen diffusion through the rapid diffusion of oxygen, high electronic conductivity, a high catalytic activity for the reduction of oxygen and a suitable thermal expansion coefficient to assure chemical and mechanical compatibility between electrode and electrolyte materials [3]. The cathodes are meant to provide high reaction rate for multistep Oxygen Reduction Reaction (ORR) which involves three phases such as, a) Electrode surface path: The oxygen species adsorbed on the surface of the cathode migrate along the electrode surface through TPB followed by complete ionization and ionic transfer to the electrolyte; b) Electrode bulk path: As the previous one, initially oxygen species will be adsorbed on the cathode surface; however in this case the species are locally dissociated, ionized and then incorporated into the bulk electrode. The transfer of oxide ions occurs through bulk electrode followed by ionization and ionic transfer to electrolyte; c) Electrolyte surface path: The oxygen species adsorbed on the electrolyte surface. It is similar to electrode surface path way unless partial ionization is accomplished by the electrolyte. Due to the smaller surface area and low ionic conductivity of most of the electrolytes, this pathway is less favored and not taken enough attention among the research groups. In most of the cases, the electrochemical reactions occur in the immediate neighboring TPBs *via* any one of these above three path ways. Perovskite type (ABO_3, A = La and other rare earth metals, Ca, Sr, Ba etc.; B = Mn, Fe, Co, Ni etc.) complex oxides are widely studied for application in SOFC due to their mixed oxygen ionic and electrical conductivities [4]. Cobaltites and manganites have better electro-catalytic activities for oxygen reduction reaction as well as higher electronic conductivities than other electrode materials [5]. Manganite based perovskite oxides such as $La_{1-x}Sr_xMnO_{3-\delta}$ (LSM) have been used widely as cathode materials for solid oxide fuel cells. These manganite based materials have relatively good stability at high temperature, however during long annealing times, pyrochlores ($La_2Zr_2O_7$) are reported to form at the boundary between LSM and yttria stabilized zirconia (YSZ). Therefore, better electrode materials that are non reactive with adjoining electrolyte are required [6]. To date, however, LSM-based composites (> 800 °C) and $La_{0.6}Sr_{0.4}Co_{0.2}Fe_{0.8}O_{3-\delta}$ (LSCF) (< 750 °C) still remain the most widely used cathodes for SOFC development; the adoption of alternative cathode materials is hindered by their unproven long-term stability and limited compatibility with electrolyte/other cell components, especially at high temperatures required for cell fabrication. In our search for alternate cathode materials which can perform equally well without any reported problems, we have studied the physico-chemical and electrical properties of $Sm_{1-x}Ce_xCoO_{3-\delta}$, $Sm_{1-x}Ce_xMnO_{3-\delta}$, $Gd_{1-x}Ce_xCoO_{3-\delta}$ and $Gd_{1-x}Ce_xMnO_{3-\delta}$ (x = 0.1 and 0.2). Various synthesis processes, such as sol-gel, gel-combustion, solid state reaction, etc. are reported to synthesize cathode materials for solid oxide fuel cells. It was known that chemical precipitation is the best method for synthesizing particles with uniform particle size [7]. Hence, we adopted simple chemical precipitation method to synthesize all these materials. Then, the prepared materials were systematically characterized by XRD, FTIR, Particle Size, SEM and EDAX techniques. The electrochemical characteristics of the above materials were studied by high temperature electrochemical impedance spectroscopy technique. The obtained results were presented and discussed in-order to use them in real SOFCs as alternate cathode materials.

EXPERIMENTAL SECTION

Preparation of SOFC cathode nanoparticles by chemical precipitation

There are various solution synthesis routes (e.g. co-precipitation, hydrothermal, sol–gel, solution polymerization, solution combustion etc.) that have been used to prepare fine mixed oxide powders in narrow particle size distribution [8]. Co-precipitation is one of these routes that uses less expensive starting materials and produces phase pure oxide ceramic powders [9]. In the present study, $Sm_{1-x}Ce_xCoO_{3-\delta}$, $Sm_{1-x}Ce_xMnO_{3-\delta}$, $Gd_{1-x}Ce_xCoO_{3-\delta}$, $Gd_{1-x}Ce_xMnO_{3-\delta}$, (x = 0.1 and 0.2) powders have been synthesized by co-precipitation route.

Appropriate quantities of Gd_2O_3/Sm_2O_3 were dissolved in minimum amount of dilute nitric acid solution and made upto 100ml with distilled water. Calculated amount of nitrate salts (cerium nitrate and manganese nitrate/cobalt nitrate) were taken and dissolved in 100ml distilled water in volumetric standard flask. The required quantity of NaOH was taken and dissolved in water in 100 mL volumetric standard flaks and which was used as the precipitating solution. The aqueous nitrate solutions ($Sm(NO_3)_3$/$Gd(NO_3)_3$, $Ce(NO_3)_3$ and $Co(NO_3)_2$ / $Mn(NO_3)_2$)

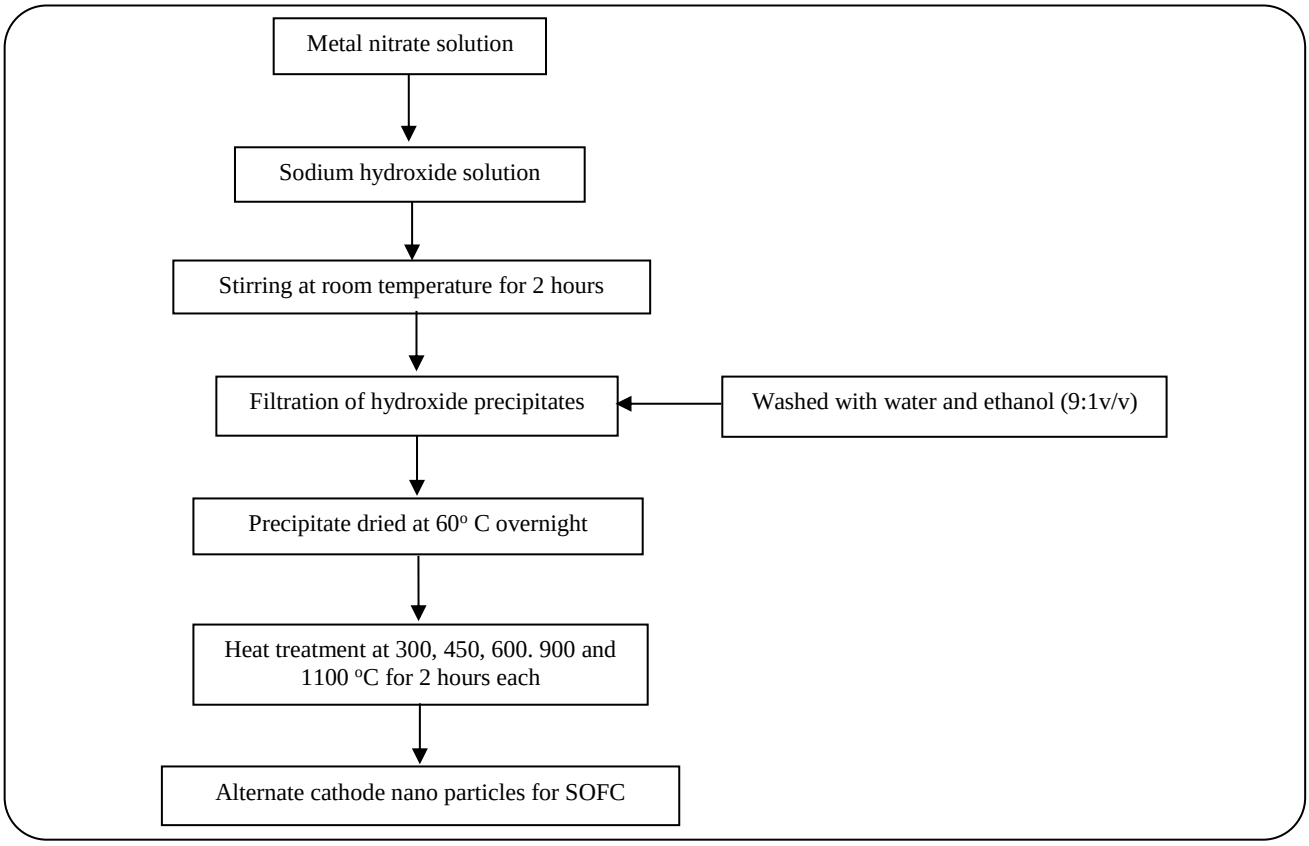

Fig.1: Schematic representation of the synthesis of alternate cathode materials by chemical precipitation method for SOFC.

were added drop wise in sequence to the sodium hydroxide solution with constant stirring with the help of magnetic stirrer and the pH was maintained above 12 by the addition of sodium hydroxide pellets during stirring. It was reported that the pH of reacting solution should be more than 12 during the course of reaction for the complex precipitation [10]. The mixture was stirred well for about 2hours. The resultant precipitate was filtered and washed thoroughly with water/ethanol mixture (9:1 v/v) and dried at 333K overnight. Then, the powdery precipitate was calcined at 300, 450, 600. 900 and 1100 ºC for 2 hours each in air to get the phase pure material. The calcined powder was ground well with pestle and mortar and subjected for further characterization. Fig. 1 shows the schematic representation of the synthesis of alternate cathode materials by chemical precipitation process.

Characterization of the samples

The heat treated powder was characterized by Shimadzu XRD 6000 X-ray diffractometer at a scan speed of 5 degrees minute^{-1} using CuKα radiation. The lattice parameters were calculated by least square fitting method using DOS computer programming. The theoretical density of the powders was calculated with the obtained XRD data. The crystallite sizes of the powder were calculated by Scherrer's formula. Bruker IFS 66V FT-IR spectrometer was employed to record the FTIR spectra of alternate cathode materials in the range of 4000-400cm^{-1}. The particle size of the powder was measured suing Malvern particles size analyzer suing triple distilled water as medium. EDAX analysis was performed with JEOL model JSM-6360 to find out the percentage of elements present in the samples. The surface morphology of the particles was studied by means of JEOL Model JSM-6360 scanning electron microscope. The prepared powders were pressed (at 3000psi) into circular specimens (8mm diameter X 1.5mm thickness) with addition of binder (Heraues V006). Then, the pressed specimens were sintered at 750º C for 5 hours in air. The electronic conductivity of these sintered specimens was obtained using two probe A.C. impedance spectroscopy. Before measurements, the specimen was pressed between two

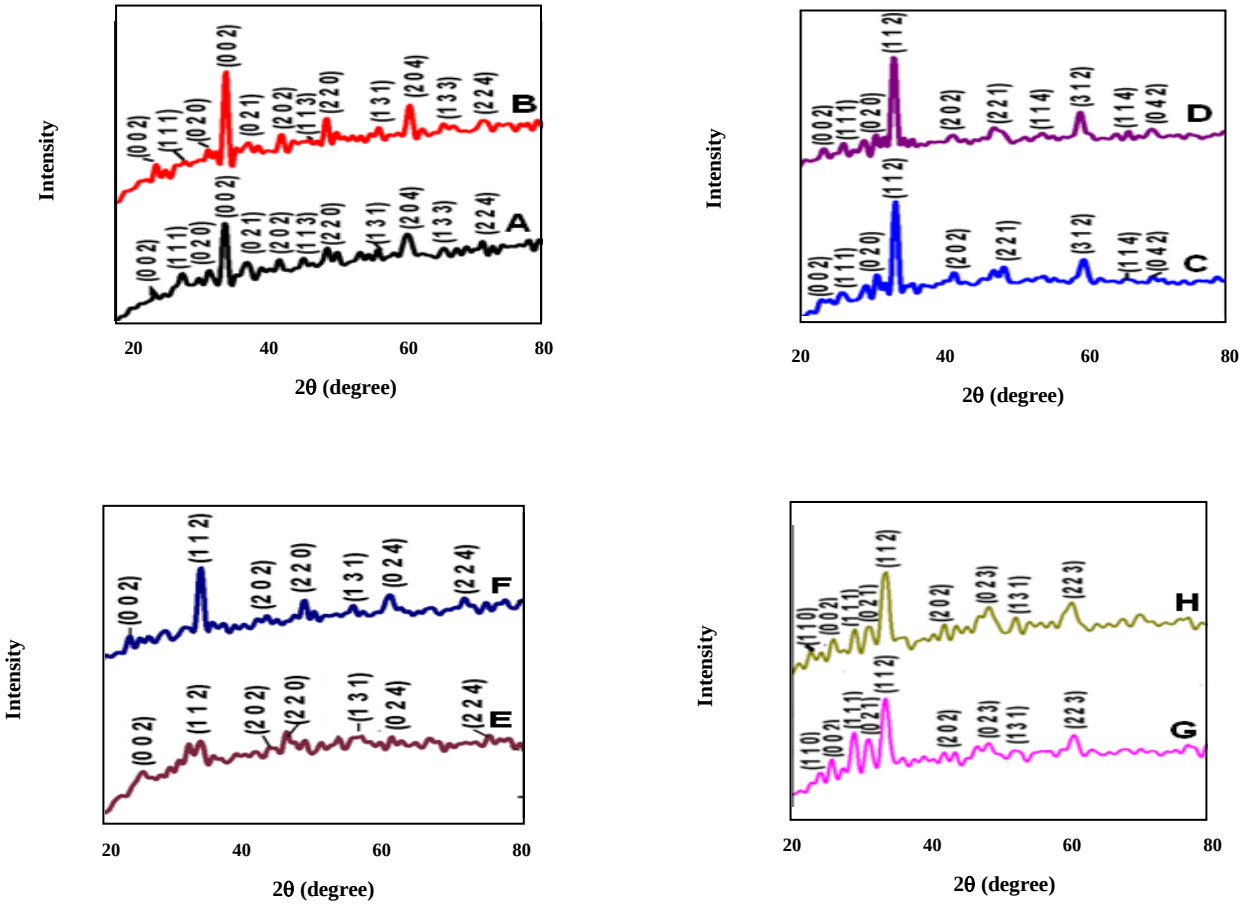

Fig. 2: XRD patterns obtained on doped cathode nanoparticles prepared by chemical precipitation method for SOFC (A) $Sm_{0.9}Ce_{0.1}CoO_{3-\delta}$, (B) $Sm_{0.8}Ce_{0.2}CoO_{3-\delta}$, (C) $Sm_{0.9}Ce_{0.1}MnO_{3-\delta}$, (D) $Sm_{0.8}Ce_{0.2}MnO_{3-\delta}$, (E) $Gd_{0.9}Ce_{0.1}CoO_{3-\delta}$, (F) $Gd_{0.8}Ce_{0.2}CoO_{3-\delta}$, (G) $Gd_{0.9}Ce_{0.1}MnO_{3-\delta}$ and (H) $Gd_{0.8}Ce_{0.2}MnO_{3-\delta}$.

golden foils. The measurements were made at 100 -750° C in air using Solatron 1260 frequency response analyzer combined with Solatron 1296 Electrochemical Interface (ECI). The standard condition followed to do the impedance measurements are voltage of 1.3V and the frequency range of 42Hz to 5kHz. The current collectors were made up of gold mesh and the current leads were platinum wires.

RESULTS AND DISCUSSION

XRD studies obtained on SOFC cathode powders

The XRD patterns of the cathode nanoparticles prepared by the chemical precipitation method for SOFC are shown in Fig. 2 (A-H). The XRD patterns of the heat treated powders reveal the formation of well-crystallined single phase materials. The XRD patterns of $Sm_{1-x}Ce_xCoO_{3-\delta}$, $Sm_{1-x}Ce_xMnO_{3-\delta}$, $Gd_{1-x}Ce_xCoO_{3-\delta}$ and $Gd_{1-x}Ce_xMnO_{3-\delta}$ were matched with the standard data for 25-1071, 25-074, 25-1057 and 25-0337 respectively and a little shift in peak position is observed in the diffraction pattern with respect to pure compounds $GdCoO_3$, $GdMnO_3$, $SmCoO_3$ and $SmMnO_3$. XRD analysis of all these samples samples suggests that they had a single phase without detectible amount of impurity after firing at 1100 °C in air for 2 hours. The crystallographic parameters obtained on the doped cathode nanoparticles for SOFC are given in Table 1. The perovskite type orthorhombic structure of $(Gd/Sm)(Co/Mn)O_3$ remains unchanged in the range of cerium substitution in all the samples. No extra peak has been observed in the diffraction pattern indicating the complete solubility of cerium in $(Gd/Sm)(Co/Mn)O_3$ perovskite phase

Table 1: Crystallographic parameters obtained on alternate cathode nanoparticles for SOFC.

Sample	Crystal structure	Unit cell lattice parameters (Å)	Unit cell volume (Å^3)	Crystallite Size (nm)
$Sm_{0.9}Ce_{0.1}CoO_{3-\delta}$	Orthorhombic	a = 5.2809; b = 5.4317; c = 7.5535	216.6	11.15
$Sm_{0.8}Ce_{0.2}CoO_{3-\delta}$	Orthorhombic	a = 5.2597; b = 5.4384; c = 7.5596	216.2	11.10
$Sm_{0.9}Ce_{0.1}MnO_{3-\delta}$	Orthorhombic	a = 5.4040; b = 5.8063; c = 7.5012	235.3	13.54
$Sm_{0.8}Ce_{0.2}MnO_{3-\delta}$	Orthorhombic	a = 5.3709; b = 5.8351; c = 7.3345	229.86	14.26
$Gd_{0.9}Ce_{0.1}CoO_{3-\delta}$	Orthorhombic	a = 5.2481; b = 5.3551; c = 7.3851	207.55	8.87
$Gd_{0.8}Ce_{0.2}CoO_{3-\delta}$	Orthorhombic	a = 5.2058; b = 5.4175; c = 7.4060	208.87	6.48
$Gd_{0.9}Ce_{0.1}MnO_{3-\delta}$	Orthorhombic	a = 5.3374; b = 5.8031; c = 7.5079	232.54	5.82
$Gd_{0.8}Ce_{0.2}MnO_{3-\delta}$	Orthorhombic	a = 5.3568; b = 5.9769; c = 7.4953	239.98	9.25

in the experimental range of substitution. As the ionic radius of Ce^{4+} is higher compared to Gd^{3+} and Sm^{3+}, an increase in cell volume is expected [11]. The crystallite size values were calculated by Scherrer's equation and reported.

FT-IR studies obtained on SOFC cathode powders

Figs. 3 (A-H) show the FTIR spectra obtained on doped cathode nanoparticles prepared by chemical precipitation method for SOFC. The broad peaks which are appeared at around 3400 cm^{-1} are related to the O-H stretching vibration of H_2O in the samples [12]. According to the standard FT-IR spectra, peaks appeared at around 800-900 cm^{-1} as well as the shoulder peaks that appear around 1400 – 1500 cm^{-1} are attributed to Ce-O vibration mode. These peaks are seen in the all prepared sample since cerium is present all samples [13, 14]. Fig. 3 (E, F, G and H) has shown peaks at 400 to 550 cm^{-1} which may be due to Gd-O bond [15, 16] and Fig. 3 (A, B, C and D) has shown a peaks at about 480-530cm^{-1} which may be due to Sm-O bond [17, 18]. The peaks appeared at 525–578, 660–670 cm^{-1} and 720-755 cm^{-1} in Fig. 3 (A,B,E and F) may be due to the stretching vibrations of the Co–O bond [19-21]. The peaks at 600-667 cm^{-1} in Fig. 3 [C, D, G and H] may be due to Mn-O bond [22]. The peak at about 2300 cm^{-1} may be due to Co-O/Mn-O bonds. The presence of perovskite phase is confirmed which is

Particle size measurements obtained on SOFC cathode powders

The prepared cathode samples ($Sm_{0.9}Ce_{0.1}CoO_{3-\delta}$, $Sm_{0.8}Ce_{0.2}CoO_{3-\delta}$, $Sm_{0.9}Ce_{0.1}MnO_{3-\delta}$, $Sm_{0.8}Ce_{0.2}MnO_{3-\delta}$, $Gd_{0.9}Ce_{0.1}CoO_{3-\delta}$, $Gd_{0.8}Ce_{0.2}CoO_{3-\delta}$, $Gd_{0.9}Ce_{0.1}MnO_{3-\delta}$ and $Gd_{0.8}Ce_{0.2}MnO_{3-\delta}$) were subjected to particle size measurements using Malvern particle size analyzer with triple distilled water as medium. For all the measurements, the samples were sonicated in triple distilled water before subjecting them for particle size measurements. The particle size distribution curves obtained on alternate cathode materials prepared by chemical precipitation method are shown in Fig. 4 (A-H). The size in nanometer is considered as x-axis and the intensity (%) of the nano particles is considered as y-axis in all the graphical representations.

From the particle characteristics data, it was understood that the average particle size of alternate cathode samples prepared by prepared chemical precipitation method reported in the range of 247-976 nm. The presence of bigger size particles may be due to the high temperature treatment [23]. However, we found that an increase in the heat treatment temperature resulted in improved crystallinity as reported in the literature [24].

Scanning Electron Microscopic (SEM) studies of SOFC cathode powders

The SEM photographs obtained on SOFC cathode powers are shown in Fig. 5 (A-H). From the SEM studies, it was found that the particles are homogeneous with the presence of highly porous structure with particle size in nm range. The presence of large sized particles in the samples may be due to the agglomeration during high temperature treatment. Also, the micrographs reveal the fluffy nature of the samples. In all the samples, well defined fine grains are uniformly distributed.

EDAX analysis

Fig. 6 (A – H) display the Energy Dispersive Analysis X-ray microanalysis (EDAX) spectra of the nanocrystalline

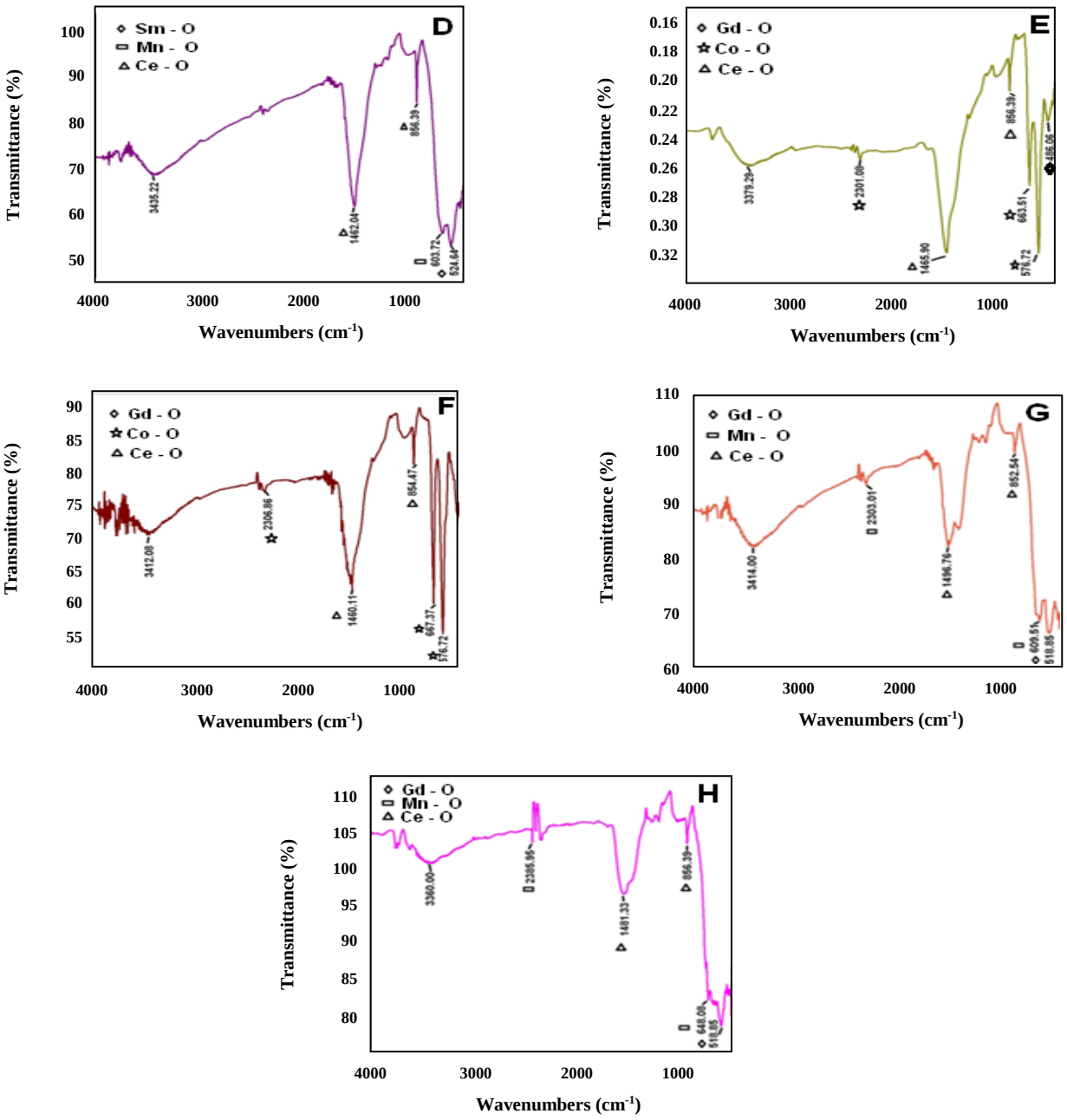

Fig. 3: FT-IR spectra obtained on doped cathode nanoparticles prepared by chemical precipitation method for SOFC (A) $Sm_{0.9}Ce_{0.1}CoO_{3-\delta}$, (B) $Sm_{0.8}Ce_{0.2}CoO_{3-\delta}$, (C) $Sm_{0.9}Ce_{0.1}MnO_{3-\delta}$, (D) $Sm_{0.8}Ce_{0.2}MnO_{3-\delta}$, (E) $Gd_{0.9}Ce_{0.1}CoO_{3-\delta}$, (F) $Gd_{0.8}Ce_{0.2}CoO_{3-\delta}$, (G) $Gd_{0.9}Ce_{0.1}MnO_{3-\delta}$ and (H) $Gd_{0.8}Ce_{0.2}MnO_{3-\delta}$.

materials ($Sm_{0.9}Ce_{0.1}CoO_{3-\delta}$, $Sm_{0.8}Ce_{0.2}CoO_{3-\delta}$, $Sm_{0.9}Ce_{0.1}MnO_{3-\delta}$, $Sm_{0.8}Ce_{0.2}MnO_{3-\delta}$, $Gd_{0.9}Ce_{0.1}CoO_{3-\delta}$, $Gd_{0.8}Ce_{0.2}CoO_{3-\delta}$, $Gd_{0.9}Ce_{0.1}MnO_{3-\delta}$ and $Gd_{0.8}Ce_{0.2}MnO_{3-\delta}$) prepared by chemical precipitation method. EDAX spectra of the samples show peaks for the elements Sm/Gd, Ce, Co/Mn and O only and not for any other impurities in the samples. The elemental composition data obtained on nanocrystalline materials by EDAX analysis is given in Table 2. The data confirmed the presence of appropriate elements in all the samples.

Electrical conductivity studies

The perovskite structures doped with transition metal oxides of Fe, Co, Mn, etc. are well known for their mixed

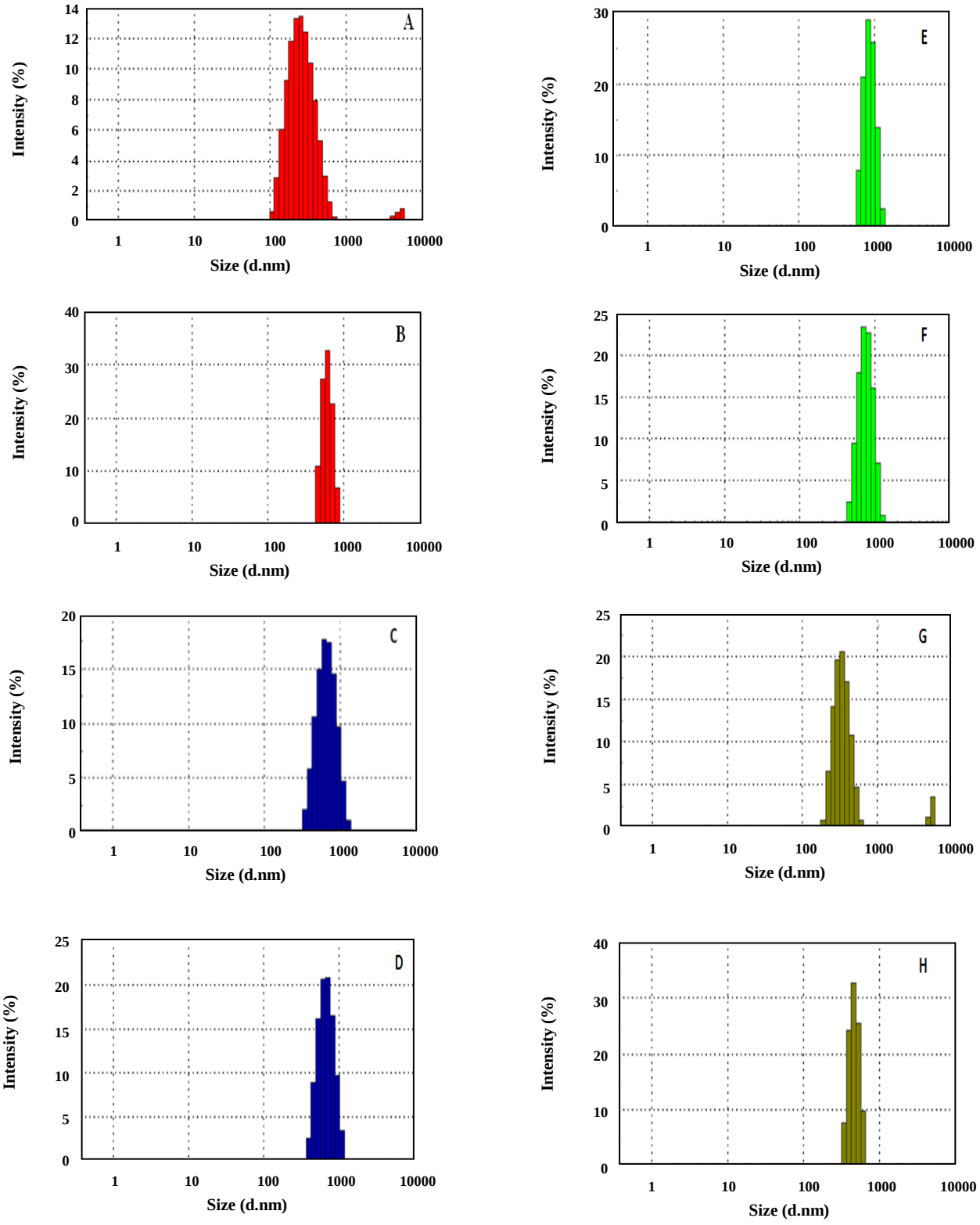

Fig. 4: Particle size patterns obtained on doped cathode nanoparticles prepared by chemical precipitation method for SOFC (A) $Sm_{0.9}Ce_{0.1}CoO_{3-\delta}$, (B) $Sm_{0.8}Ce_{0.2}CoO_{3-\delta}$, (C) $Sm_{0.9}Ce_{0.1}MnO_{3-\delta}$, (D) $Sm_{0.8}Ce_{0.2}MnO_{3-\delta}$, (E) $Gd_{0.9}Ce_{0.1}CoO_{3-\delta}$, (F) $Gd_{0.8}Ce_{0.2}CoO_{3-\delta}$, (G) $Gd_{0.9}Ce_{0.1}MnO_{3-\delta}$ and (H) $Gd_{0.8}Ce_{0.2}MnO_{3-\delta}$.

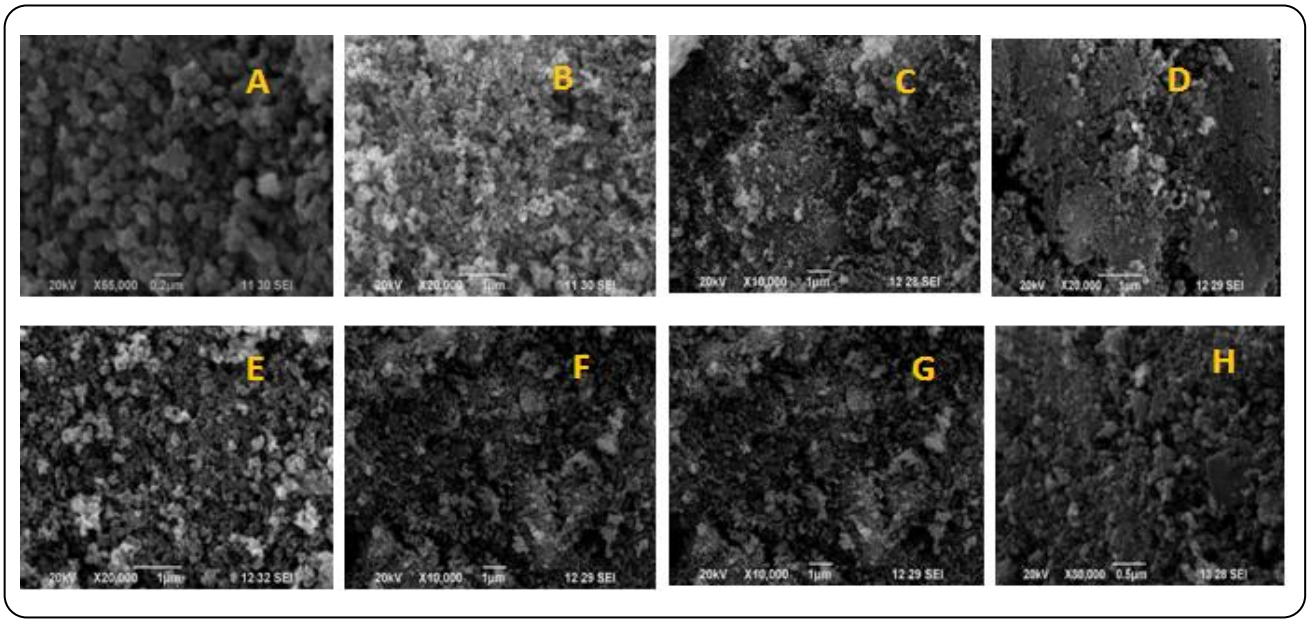

Fig. 5: SEM photographs obtained on doped cathode nanoparticles prepared by chemical precipitation method for SOFC (A) $Sm_{0.9}Ce_{0.1}CoO_{3-\delta}$, (B) $Sm_{0.8}Ce_{0.2}CoO_{3-\delta}$, (C) $Sm_{0.9}Ce_{0.1}MnO_{3-\delta}$, (D) $Sm_{0.8}Ce_{0.2}MnO_{3-\delta}$, (E) $Gd_{0.9}Ce_{0.1}CoO_{3-\delta}$, (F) $Gd_{0.8}Ce_{0.2}CoO_{3-\delta}$, (G) $Gd_{0.9}Ce_{0.1}MnO_{3-\delta}$ and (H) $Gd_{0.8}Ce_{0.2}MnO_{3-\delta}$.

ionic and electronic conductivity properties [25]. Sufficient electrical conductivity is the major parameter for better performance of cathode material. The SOFC cathode materials such as $Sm_{0.9}Ce_{0.1}CoO_{3-\delta}$, $Sm_{0.8}Ce_{0.2}CoO_{3-\delta}$, $Sm_{0.9}Ce_{0.1}MnO_{3-\delta}$, $Sm_{0.8}Ce_{0.2}MnO_{3-\delta}$, $Gd_{0.9}Ce_{0.1}CoO_{3-\delta}$, $Gd_{0.8}Ce_{0.2}CoO_{3-\delta}$, $Gd_{0.9}Ce_{0.1}MnO_{3-\delta}$ and $Gd_{0.8}Ce_{0.2}MnO_{3-\delta}$ were subjected electrical conductivity measurements as mentioned below. The prepared powders were pressed (at 3000 psi) into disk type specimens (8 mm diameter x 1.5 mm thickness) with addition of binder.

Then, the pressed specimens were sintered at 800 ^{o}C for 5 hours in air. Both sides of the pellets were coated with silver paste before subjecting the samples for electrical conductivity measurements. Fig. 7 (A-H) show the AC impedance spectra obtained for alternate cathode specimens at different temperatures. The frequency range for all the spectra was found to be less than 200kHz. From the plots, it was noted that as the temperature is increased, the time constants of the relaxations resulting from the individual polarizations are reduced and the arcs are shifted to higher frequencies as reported in literature [26]. Because of this, the conductivity of the sintered tends to increase with increase in temperature. This behavior is consistent with small polaron conduction (localized electronic carriers having a thermally activated mobility). The increase is much more pronounced for samples with higher densities, i.e., when sintering temperature is higher [27, 28]. From the impedance plots, the individual resistance R_i can be converted to conductivity, σ_i using the equation $\sigma_i = L/SR_i$, where 'L' is the sample thickness and 'S' the electrode area of the sample surface. The conductivity values for all the cathode specimens were calculated and reported in Table 3.

It is clear from the electrochemical characterization that the electrical conductivity gradually improves with the increase of temperature, which primarily reflects the property of electronic conduction of the perovskite based materials. Among the samples studied, $Gd_{0.8}Ce_{0.2}CoO_{3-\delta}$ resulted in better performance and resulted in optimal conductivity value. This may be due to good sintering of the materials than other samples. Another possible explanation could be due to surface diffusion mechanism and this is related to the perfect microstructure of the material. Another reason could be due to optimized surface phenomenon in the perovskite lattice [29]. However, the sintering temperature and other relevant physico-chemical parameters need to be further optimized for considering the proposed materials as alternative cathodes for LTSOFC application.

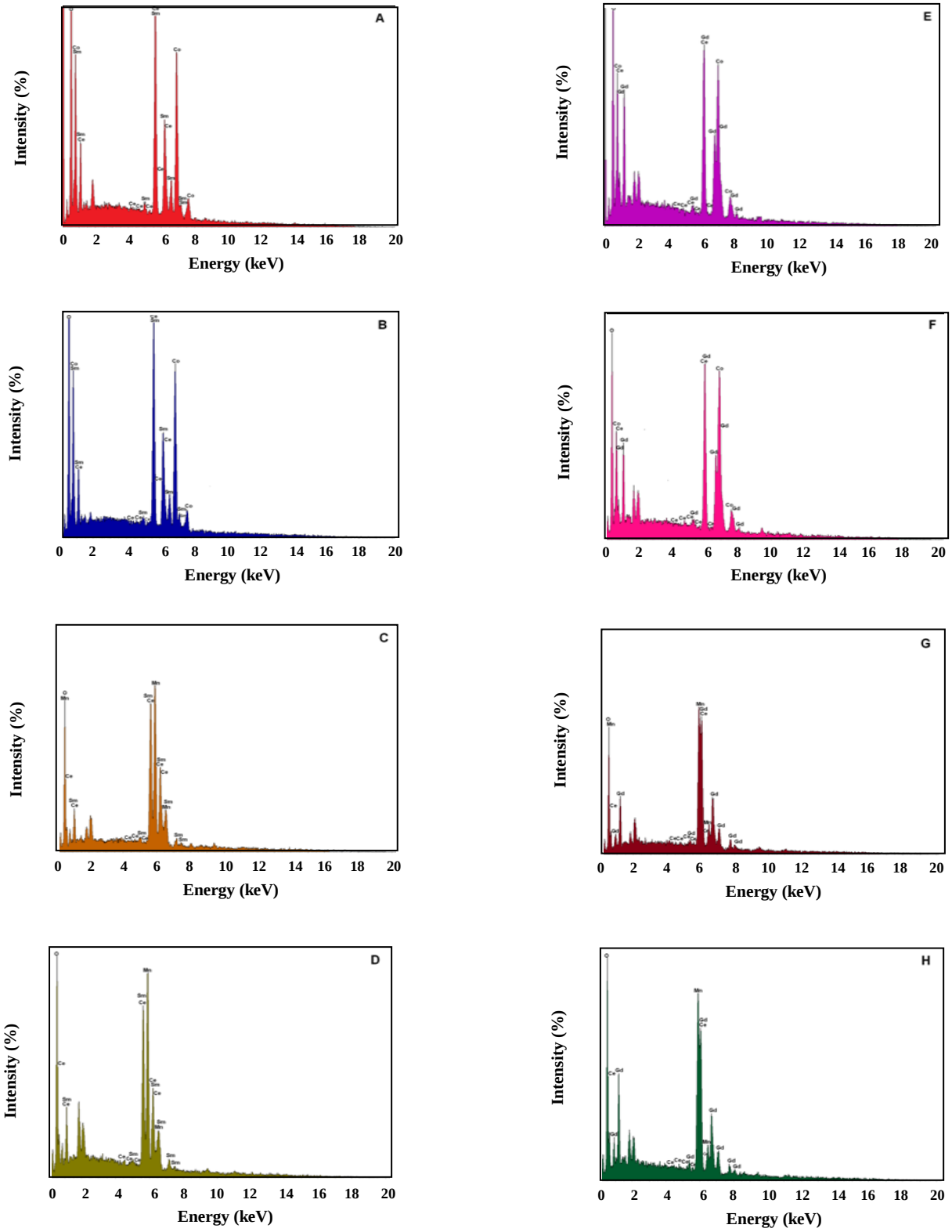

Fig. 6: EDAX spectra obtained on doped cathode nanoparticles prepared by chemical precipitation method for SOFC (A) $Sm_{0.9}Ce_{0.1}CoO_{3-\delta}$, (B) $Sm_{0.8}Ce_{0.2}CoO_{3-\delta}$, (c) $Sm_{0.9}Ce_{0.1}MnO_{3-\delta}$,(D) $Sm_{0.8}Ce_{0.2}MnO_{3-\delta}$, (E) $Gd_{0.9}Ce_{0.1}CoO_{3-\delta}$, (F) $Gd_{0.8}Ce_{0.2}CoO_{3-\delta}$, (G) $Gd_{0.9}Ce_{0.1}MnO_{3-\delta}$ (H) $Gd_{0.8}MnCe_{0.2}CoO_{3-\delta}$.

Table 2: Elemental composition data obtained on alternate cathode materials for SOFC.

Sample	Elements	Atomic weight percentage
$Sm_{0.9}Ce_{0.1}CoO_{3-\delta}$	O	26.01
	Co	24.32
	Ce	0.32
	Sm	49.35
$Sm_{0.8}Ce_{0.2}CoO_{3-\delta}$	O	24.18
	Co	25.46
	Ce	0.49
	Sm	49.27
$Sm_{0.9}Ce_{0.1}MnO_{3-\delta}$	O	19.43
	Mn	28.27
	Ce	0.03
	Sm	52.27
$Sm_{0.8}Ce_{0.2}MnO_{3-\delta}$	O	23.02
	Mn	27.74
	Ce	0.83
	Sm	48.41
$Gd_{0.9}Ce_{0.1}CoO_{3-\delta}$	O	24.61
	Co	23.53
	Ce	0.06
	Gd	51.80
$Gd_{0.8}Ce_{0.2}CoO_{3-\delta}$	O	20.21
	Co	27.10
	Ce	0.72
	Gd	51.97
$Gd_{0.9}Ce_{0.1}MnO_{3-\delta}$	O	20.28
	Mn	24.03
	Ce	0.31
	Gd	55.38
$Gd_{0.8}Ce_{0.2}MnO_{3-\delta}$	O	26.58
	Mn	23.40
	Ce	0.09
	Gd	49.92

Table 3: Electrical properties obtained on sintered doped cathode specimens for SOFC.

Sample	Temperature (° C)	Electrical Conductivity (Sm^{-1})
$Sm_{0.9}Ce_{0.1}CoO_{3-\delta}$	100	5.0339×10^{-4}
	200	2.00019×10^{-3}
	300	4.75×10^{-3}
$Sm_{0.8}Ce_{0.2}CoO_{3-\delta}$	100	4.99×10^{-3}
	200	6.2762×10^{-3}
	300	6.89×10^{-3}
$Sm_{0.9}Ce_{0.1}MnO_{3-\delta}$	100	7.426×10^{-4}
	200	8.889×10^{-3}
	300	6.68×10^{-2}
$Sm_{0.8}Ce_{0.2}MnO_{3-\delta}$	100	1.06566×10^{-3}
	200	1.2586×10^{-2}
	300	6.4935×10^{-2}
$Gd_{0.9}Ce_{0.1}CoO_{3-\delta}$	100	1.956×10^{-3}
	200	4.355×10^{-3}
	300	1.29×10^{-2}
$Gd_{0.8}Ce_{0.2}CoO_{3-\delta}$	100	1.586×10^{-2}
	200	1.05×10^{-1}
	300	7.918×10^{-1}
$Gd_{0.9}Ce_{0.1}MnO_{3-\delta}$	100	4.2×10^{-4}
	200	2.3×10^{-3}
	300	2.6×10^{-2}
$Gd_{0.8}Ce_{0.2}MnO_{3-\delta}$	100	3.8×10^{-4}
	200	5.235×10^{-3}
	300	3.4×10^{-2}

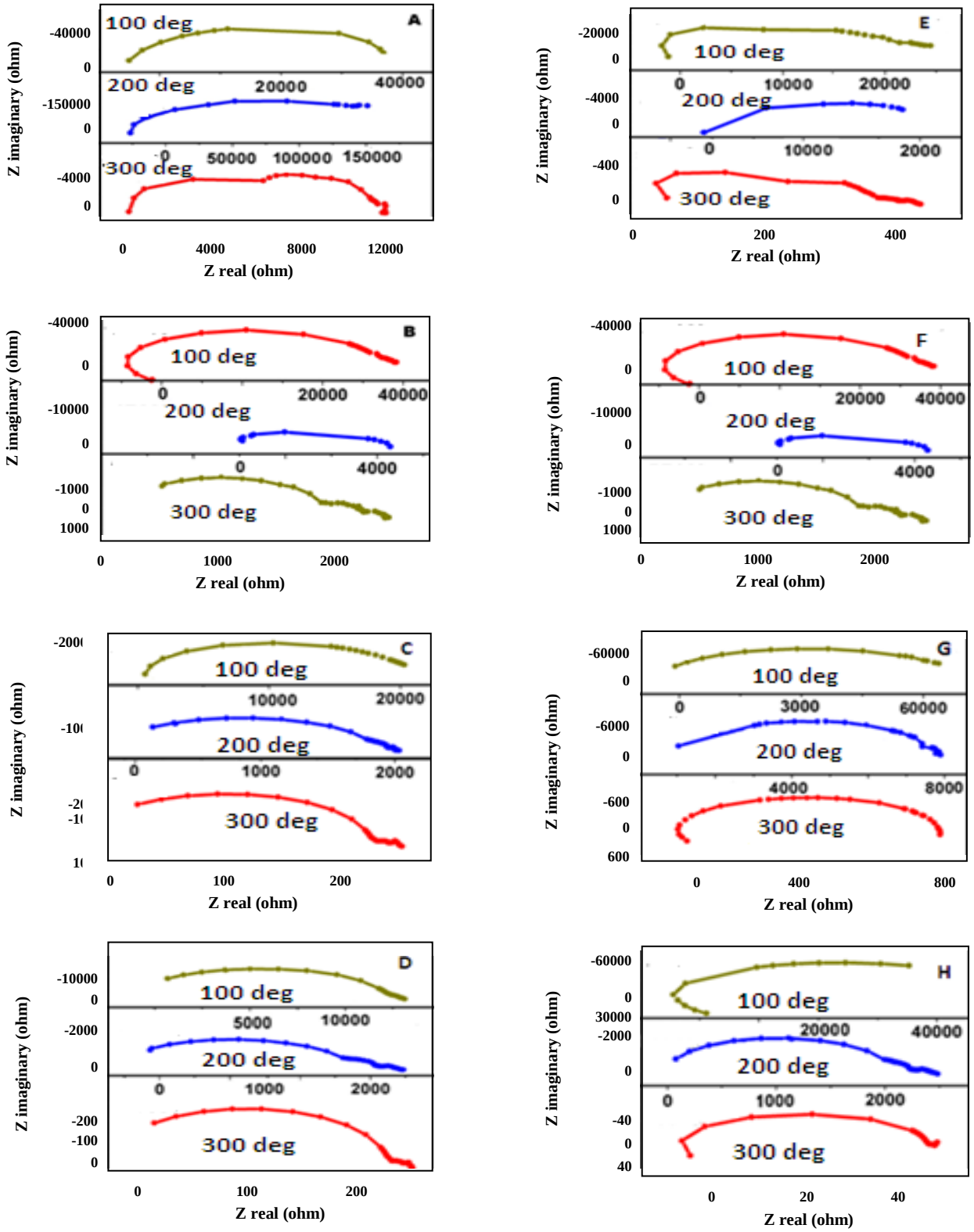

Fig. 7: AC impedance spectra obtained on sintered doped cathode specimen at different temperatures - (A) $Sm_{0.9}Ce_{0.1}CoO_{3-\delta}$, (B) $Sm_{0.8}Ce_{0.2}CoO_{3-\delta}$, (c) $Sm_{0.9}Ce_{0.1}MnO_{3-\delta}$,(D) $Sm_{0.8}Ce_{0.2}MnO_{3-\delta}$, (E) $Gd_{0.9}Ce_{0.1}CoO_{3-\delta}$, (F) $Gd_{0.8}Ce_{0.2}CoO_{3-\delta}$, (G) $Gd_{0.9}Ce_{0.1}MnO_{3-\delta}$ (H) $Gd_{0.8}MnCe_{0.2}CoO_{3-\delta}$.

CONCLUSIONS

The chemical precipitation process can be effectively used for the preparation of phase pure alternate cathode materials for SOFC such as $Sm_{1-x}Ce_xCoO_{3-\delta}$, $Sm_{1-x}Ce_xMnO_{3-\delta}$, $Gd_{1-x}Ce_xCoO_{3-\delta}$, and $Gd_{1-x}Ce_xMnO_{3-\delta}$ (x = 0.1–0.2) using cheap chemicals. The powder XRD data obtained on doped cathode nanoparticles is in good agreement with the standard reported JCPDS data. All the samples have an orthorhombic crystal structure. FT-IR spectra confirmed the presence of metal-oxygen bond in all the samples. Particle size measurements have shown the particles in the range of 247-976 nm. The presence of microparticles may be due to the agglomeration of smaller particles at high temperatures. SEM data have shown the presence of grains in the range of 200-500nm. SEM pictures have shown the fluffy-like behavior in all the samples. EDAX data has provided an idea about the atomic weight percentage of the elements present in the samples. The alternate cathode specimens have shown an increase in conductivity concerning temperature. The cathode specimen, $Gd_{0.8}Ce_{0.2}CoO_{3-\delta}$ resulted in better performance. Hence, this may be a good choice of cathode for SOFC application.

Acknowledgments

ASN would like to thank the Central Power Research Institute (Ministry of Power, Govt. of India) (Grant No. CPRI/ R&D/ TC/ GDEC/ 2019, dated 06-02-2019) for providing financial support for SOFC research. ASN also thanks Karunya Institute of Technology and Sciences for providing the necessary facilities.

Received : Sep. 5, 2019 ; Accepted : Dec. 2, 2019

REFERENCES

[1] Sammes N., Du Y., Intermediate-Temperature SOFC Electrolytes, *Fuel Cell Technologies: State and Perspectives NATO Science Series*, **202**: 19-34 (2005).

[2] Liangdong Fan, Bin Zhu, Pei-Chen Su, Chuanxin He, Nanomaterials and Technologies for Low-Temperature Solid Oxide Fuel Cells: Recent Advances, Challenges and Opportunities, *Nano Energy*, **45**: 148-176 (2018)

[3] Ellen Ivers-Tiffée, Andre Weber, Dirk Herbstritt, Materials and Technologies for SOFC-Components, *Journal of the European Ceramic Society*, **21 (10-11)**: 1805–1811 (2001).

[4] Yaremchenkoa, Shaulaa A.L., Logvinovich D.I., Kharton V.V., Kovalevsky A.V., Naumovich E.N., Frade J.R., Marques F.M.B., Oxygen-Ionic Conductivity of Perovskite-Type $La_{1-x}Sr_xGa_{1-y}Mg_yM_{0.20}O_{3-\delta}$ (M=Fe, Co, Ni), *Materials Chemistry and Physics*, **82(3)**: 684–690 (2003).

[5] Manoj K. Mahapatra, Sanjit Bhowmick, Na Li, Prabhakar Singh, Role of Oxygen Pressure on the Stability of Lanthanum Strontium Manganite–Yttria Stabilized Zirconia Composite, *Journal of the European Ceramic Society*, **32(10)**: 2341–2349 (2012).

[6] Kharton V.V., Figueiredo F.M., Navarro L., Naumovich E.N., Kovalevsky A.V., Yaremchenko A.A., Viskup A.P., Carneiro A., Marques F.M.B., Frade J.R., Ceria-Based Materials for Solid Oxide Fuel Cells, *Journal of Materials Science*, **36(5)**: 1105-1117 (2001).

[7] Jasmine Ketzial J., Samson Nesaraj A., Synthesis of CeO_2 Nanoparticles by Chemical Precipitation and The Effect of a Surfactant on the Distribution of Particle Sizes, *Journal of Ceramic Processing Research*, **12(1)**: 74-79 (2011).

[8] Lenka R.K., Mahata T., Patroa P.K., Tyagi A.K., Sinha P.K., Synthesis and Characterization of $GdCoO_3$ as a Potential SOFC Cathode Material, *Journal of Alloys and Compounds*, **537**: 100–105 (2012).

[9] Fuentesa R.O., Baker R.T., Synthesis and Properties of Gadolinium-Doped Ceria Solid Solutions for IT-SOFC Electrolytes, *International Journal of Hydrogen Energy*, **33**(13): 3480–3484 (2002).

[10] Yaremchenko A. A., A.L Shaula, A.L., Logvinovich, D.I., Kharton V.V., Kovalevsky A.V., Naumovich E.N., Frade J.R., Marques F.M.B., Oxygen-Ionic Conductivity of Perovskite-Type $La_{1-x}Sr_xGa_{1-y}Mg_yM_{0.20}O_{3-\delta}$ (M=Fe, Co, Ni), *Materials Chemistry and Physics*, **82(3)**: 684–690 (2003).

[11] Hayashi H., Inaba H., Matsuyam M., Lan N.G., Dokiya M., Tagawa H., Structural Consideration on the Ionic Conductivity of Perovskite-Type Oxides, *Solid State Ionics*, **122(1-4)**: 1–15 (1999).

[12] Rajendran V., Gnanam S., Preparation of Pure and Pd–Doped Ceria Nanoparticles *via* Precipitation Method and Their Optical Properties, *International Journal of Nanoparticles*, **5(3)**: 267-278 (2012).

[13] Ashwani Sharma, Pallavi Sanjay Kumar, Synthesis and Characterization of CeO-ZnO Nanocomposites, *Nanoscience and Nanotechnology*, **2(3)**: 82-85 (2012).

[14] Shi-You H., Lu, Tian-Xi L., Microwave-induced Combustion Synthesis and Characterization of Porous Nanocrystalline Ce-M-O (M＝La, Pr) Powders, *Acta Chemica Sinica*, **66(10)**: 1203-1208 (2008).

[15] Liu G., Hong G., Wang J., Dong X., Deposition of $GdVO_4$: Eu^{3+} Nanoparticles on Silica Nanospheres by a Simple Sol-Gel Method, *Nanotechnology*, **17**: 3134-3138 (2006).

[16] Li G. Z., Yu M., Wang Z. L., Lin J., Wang R. S., Fang J., Sol-Gel Fabrication and Photoluminescence Properties of SiO2 @ Gd2O3: Eu3+ Core-Shell Particles, *Journal of Nanoscience and Nanotechnology*, **6(5)**: 1416-1422 (2006).

[17] Fan X,, Shang K., Sun B., Chen L., Ai S., Decoration of Surface-Carboxylated Graphene Oxide with Luminescent Sm^{3+}-Complexes, *Journal of Materials Science*, **49(6)**: 2672-2679 (2014).

[18] Miguel A.Ruiz-Gómez, ChristianGómez-Solís, María E., Zarazúa-Morín, Leticia M.Torres-Martínez, IsaíasJuárez-Ramírez, DanielSánchez-Martínez, Mayra Figueroa-Torres Z., Innovative Solvo-Combustion Route For The Rapid Synthesis of MoO_3 and Sm_2O_3 Materials, *Ceramics International*, **40(1)**: 1893–1899 (2014).

[19] Rohith P. John, A. Sreekanth, Maliyeckal R., Prathapachandra Kurup, Shaikh M Mobin, Synthesis and Structural Studies of Novel Co(III) Ternary Complexes Containing N(4)-Substituted Thiosemicarbazones of 2-Hydroxyacetophenone and Heterocyclic Bases, *Polyhedron*, **21(24)**: 2515–2521 (2002).

[20] Suresh P., Rodrigues S., Shukla A.K., Vasan H.N., Munichandraiah N., Synthesis of $LiCo_{1-x}Mn_xO_2$ from a Low-Temperature Route and Characterization as Cathode Materials in Li-Ion Cells, *Solid State Ionics*, **176(3-4)**: 281–290 (2005).

[21] Chen-Bin Wang, Chih-Wei Tang, Shiue-Jiun Gau, Shu-Hua Chien, Effect of the Surface Area of Cobaltic Oxide on Carbon Monoxide Oxidation, *Catalysis Letters*, **101 (1-2)**: 59-63 (2005).

[22] Yinhua Li, Jian Gong, Gaohong He, Yulin Deng, Synthesis of Polyaniline Nanotubes Using Mn_2O_3 Nanofibers as Oxidant and their Ammonia Sensing Properties, *Synthetic Metals*, **161(1-2)**: 56–61 (2011).

[23] Rivas J., Hueso L.E., Fondado A., Rivadulla F., López-Quintela M.A., Low Field Magneto Resistance Effects in Fine Particles of Lanthanum Perovskites, *Journal of Magnetism and Magnetic Materials*, **221(1)**: 1-2 (2000)

[24] Siti Hajar Othman, Suraya Abdul Rashid, Tinia Idaty Mohd Ghazi, Norhafizah Abdullah, Effect of Postdeposition Heat Treatment on the Crystallinity, Size, and Photocatalytic Activity of TiO_2 Nanoparticles Produced *Via* Chemical Vapour Deposition, *Journal of Nanomaterials*, Article ID 512785 (2010).

[25] Suman C.K., Prasad K., Choudhary R.N.P., Impedance Analysis of $Pb_2Sb_3LaTi_5O_{18}$ Ceramic, *Bulletin of Material Science*, **27(6)**: 547–553 (2004).

[26] Zhongliang Z., Ting L.W., Hengyong T., Zhi Y.L., AC Impedance Investigation of Samarium-Doped Ceria, *Journal of Electrochemical Society*, **148(5)**: L 427 – 432 (2001).

[27] Jurado R., Present Several Items on Ceria-Based Ceramic Electrolytes: Synthesis, Additive Effects, Reactivity and Electrochemical Behavior, *Journal of Materials Science*, **36(5)**: 1133-1139 (2001).

[28] Leandroda Conceição, Amanda M.Silva, Nielson F.P.Ribeiro, Mariana M.V.M.Souza, Combustion Synthesis of $La_{0.7}Sr_{0.3}Co_{0.5}Fe_{0.5}O_3$ (LSCF) Porous Materials for Application as Cathode in IT-SOFC, *Materials Research Bulletin*, **46(2)**: 308- 314 (2011).

[29] Kammer Hansen K., Hansen, K.V., Mogensen M.B., High-Performance Fe-Co Based SOFC Cathodes, *Journal of Solid State Electrochemistry*, **14(11)**: 2107–2112 (2010).